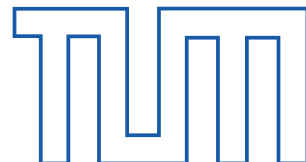


Quarkonium interactions in hadronic and nuclear matter

Wai Kin Lai

Yu Jia (PI) & Antonio Vairo (PI)

Technische Universität München



Project B.8 of the CRC110

Principal Investigators: Antonio Vairo (TUM) and Yu Jia (CAS)

Funding: 2 years post-doc (starting fall 2016) → [Wai Kin Lai](#)

Research

1. Quarkonium Production

1.1 $e^+e^- \rightarrow \chi_{cJ} + \gamma$

1.2 $H \rightarrow J/\psi + \gamma$

2. Quarkonium-Quarkonium interaction

2.1 Van der Waals EFTs in QED

2.2 Van der Waals EFTs in QCD

2.3 Chiral corrections to the quarkonium mass

3. Quarkonium interaction with light degrees of freedom

3.1 Born–Oppenheimer EFT in QED

3.2 Born–Oppenheimer EFT in QCD (see project A3)

1. Quarkonium Production

1.1 Quarkonium production in $e^+e^- \rightarrow \chi_{cJ} + \gamma$

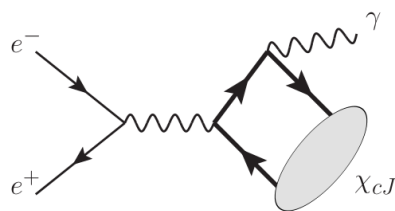
Authors: Nora Brambilla (TUM) Wen Chen (CAS) Yu Jia (CAS)
Vladyslav Shtabovenko (TUM) Antonio Vairo (TUM)

Report: TUM-EFT 68/15

→ see talk of [Wen Chen](#) for an extended presentation.

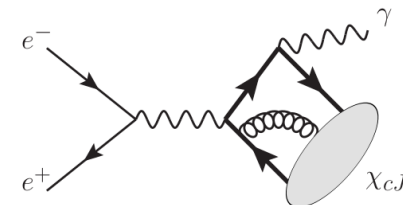
1.1 Motivation

- ▶ Electromagnetic spin triplet P -wave quarkonium production in e^+e^- -annihilation: γ^* decays into a hard on-shell γ and a χ_{cJ} :



- ▶ No experimental data available, good perspectives for this measurement will exist at Belle II in Japan
- ▶ An early study [Chung et al., 2008] based on $\mathcal{O}(\alpha_s^0 v^0)$ results predicted cross-sections that might be measurable at B-factories (here for $\sqrt{s} = 10.6$ GeV):
 - ★ $\sigma(e^+e^- \rightarrow \chi_{c0} + \gamma) = 1.3$ fb
 - ★ $\sigma(e^+e^- \rightarrow \chi_{c1} + \gamma) = 13.7$ fb
 - ★ $\sigma(e^+e^- \rightarrow \chi_{c2} + \gamma) = 5.3$ fb
- ▶ Subsequently, corrections of order $\mathcal{O}(\alpha_s v^0)$ ([Sang & Chen, 2010], [Li et al., 2009]), $\mathcal{O}(\alpha_s^0 v^2)$ ([Li et al., 2013], [Chao et al., 2013]) and finally $\mathcal{O}(\alpha_s v^2)$ ([Xu et al., 2014]) were obtained as well.

- ▶ C.f. also treatment in the light cone formalism ([Braguta, 2010] [Wang & Yang, 2014])
- ▶ So far, all the previous NRQCD studies were concerned with the operators that contribute through the dominant Fock state $|Q\bar{Q}\rangle$.
- ▶ However, at $\mathcal{O}(v^2)$ operators that contribute through the subleading Fock state $|Q\bar{Q}g\rangle$ show up as well \Rightarrow CO mechanism of NRQCD.



- ▶ The availability of the CS $\mathcal{O}(\alpha_s^0 v^2)$ corrections suggests that CO $\mathcal{O}(\alpha_s^0 v^2)$ corrections should be determined as well.

1.1 NRQCD factorization

Exclusive production of χ_{cJ} in NRQCD at $\mathcal{O}(v^2)$

$$\sigma(e^+e^- \rightarrow \chi_{c0} + \gamma) = \frac{F_1(^3P_0)}{m^4} \langle 0 | \mathcal{O}_1(^3P_0) | 0 \rangle + \frac{G_1(^3P_0)}{m^6} \langle 0 | \mathcal{P}_1(^3P_0) | 0 \rangle + \frac{T_8(^3P_0)}{m^5} \langle 0 | \mathcal{T}_8(^3P_0) | 0 \rangle$$

$$\sigma(e^+e^- \rightarrow \chi_{c1} + \gamma) = \frac{F_1(^3P_1)}{m^4} \langle 0 | \mathcal{O}_1(^3P_1) | 0 \rangle + \frac{G_1(^3P_1)}{m^6} \langle 0 | \mathcal{P}_1(^3P_1) | 0 \rangle + \frac{T_8(^3P_1)}{m^5} \langle 0 | \mathcal{T}_8(^3P_1) | 0 \rangle$$

$$\sigma(e^+e^- \rightarrow \chi_{c2} + \gamma) = \frac{F_1(^3P_2)}{m^4} \langle 0 | \mathcal{O}_1(^3P_2) | 0 \rangle + \frac{G_1(^3P_2)}{m^6} \langle 0 | \mathcal{P}_1(^3P_2) | 0 \rangle + \frac{T_8(^3P_2)}{m^5} \langle 0 | \mathcal{T}_8(^3P_2) | 0 \rangle$$

Production LDMEs

$$\langle 0 | \mathcal{O}_1(^3P_0) | 0 \rangle \equiv \frac{1}{3} \langle 0 | \chi^\dagger \left(-\frac{i}{2} \overset{\leftrightarrow}{\mathbf{D}} \cdot \boldsymbol{\sigma} \right) \psi | \chi_{c0} \rangle \times \\ \langle \chi_{c0} | \psi^\dagger \left(-\frac{i}{2} \overset{\leftrightarrow}{\mathbf{D}} \cdot \boldsymbol{\sigma} \right) \chi | 0 \rangle$$

$$\langle 0 | \mathcal{P}_1(^3P_0) | 0 \rangle \equiv \frac{1}{6} \left(\langle 0 | \chi^\dagger \left(-\frac{i}{2} \overset{\leftrightarrow}{\mathbf{D}} \cdot \boldsymbol{\sigma} \right) \psi | \chi_{c0} \rangle \times \right. \\ \left. \langle \chi_{c0} | \psi^\dagger \left(-\frac{i}{2} \overset{\leftrightarrow}{\mathbf{D}} \cdot \boldsymbol{\sigma} \right) \left(-\frac{i}{2} \overset{\leftrightarrow}{\mathbf{D}} \right)^2 \chi | 0 \rangle + \text{h.c.} \right)$$

$$\langle 0 | \mathcal{T}_8(^3P_0) | 0 \rangle \equiv \frac{1}{6} \left(\langle 0 | \chi^\dagger \left(\overset{\leftrightarrow}{\mathbf{D}} \cdot \boldsymbol{\sigma} \right) \psi | \chi_{c0} \rangle \times \right. \\ \left. \langle \chi_{c0} | \psi^\dagger (g \mathbf{E} \cdot \boldsymbol{\sigma}) \chi | 0 \rangle + \text{h.c.} \right)$$

Scaling

- In the power-counting of [Bodwin et al., 1995] we have

$$\langle 0 | \mathcal{O}_1(^3P_J) | 0 \rangle \sim v^5$$

$$\langle 0 | \mathcal{P}_1(^3P_J) | 0 \rangle \sim \langle 0 | \mathcal{T}_8(^3P_J) | 0 \rangle \sim v^7$$

- Once we include contributions from $\langle 0 | \mathcal{P}_1(^3P_J) | 0 \rangle$, we must also include $\langle 0 | \mathcal{T}_8(^3P_J) | 0 \rangle$!

Notation

- **bold font** denotes Cartesian 3-vectors
- ψ (χ) annihilates (creates) a heavy quark (antiquark)
- $\boldsymbol{\sigma}$ is the Pauli vector
- $\mathbf{D} \equiv \nabla - ig\mathbf{A}$
- \mathbf{A} is the gluon field
- \mathbf{E} is the chromoelectric field
- $\psi^\dagger \overset{\leftrightarrow}{\mathbf{D}} \chi \equiv \psi^\dagger (\mathbf{D}\chi) - (\mathbf{D}\psi)^\dagger \chi$

1.1 Analytical results

Final results (including the known $\mathcal{O}(\alpha_s v^0)$ [Sang & Chen, 2010, Li & Chao, 2009] correction to $F_1(^3P_J)$)

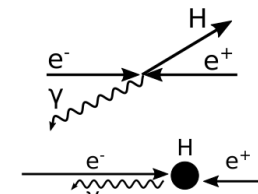
$$\begin{aligned}\sigma(e^+e^- \rightarrow \chi_{c0} + \gamma) &= \frac{(4\pi\alpha)^3 e_Q^4 (1-3r)^2}{18\pi m^3 s^2 (1-r)} \left\{ \left(1 + \frac{\alpha_s}{\pi} C_0^0(r) \right) \langle 0 | \mathcal{O}_1(^3P_0) | 0 \rangle \right. \\ &\quad \left. - \frac{(13-18r+25r^2)}{10m^2(1-4r+3r^2)} \langle 0 | \mathcal{P}_1(^3P_0) | 0 \rangle + \frac{2r(2-3r)}{m(1-4r+3r^2)} \langle 0 | \mathcal{T}_8(^3P_0) | 0 \rangle \right\}, \\ \sigma(e^+e^- \rightarrow \chi_{c1} + \gamma) &= \frac{(4\pi\alpha)^3 e_Q^4 (1+r)}{3\pi m^3 s^2 (1-r)} \left\{ \left(1 + \frac{\alpha_s}{\pi} \frac{C_1^0(r) + rC_1^1(r)}{1+r} \right) \langle 0 | \mathcal{O}_1(^3P_1) | 0 \rangle \right. \\ &\quad \left. - \frac{(11-20r-11r^2)}{10m^2(1-r^2)} \langle 0 | \mathcal{P}_1(^3P_1) | 0 \rangle - \frac{(3-3r-4r^2)}{2m(1-r^2)} \langle 0 | \mathcal{T}_8(^3P_1) | 0 \rangle \right\}, \\ \sigma(e^+e^- \rightarrow \chi_{c2} + \gamma) &= \frac{(4\pi\alpha)^3 e_Q^4 (1+3r+6r^2)}{9\pi m^3 s^2 (1-r)} \left\{ \right. \\ &\quad \times \left(1 + \frac{\alpha_s}{\pi} \frac{C_2^0(r) + 3rC_2^1(r) + 6r^2C_2^2(r)}{1+3r+6r^2} \right) \langle 0 | \mathcal{O}_1(^3P_2) | 0 \rangle \\ &\quad \left. - \frac{(1+4r-30r^2)}{10m^2(1+3r+6r^2)} \langle 0 | \mathcal{P}_1(^3P_2) | 0 \rangle - \frac{(3+r-6r^2-18r^3)}{2m(1-r)(1+3r+6r^2)} \langle 0 | \mathcal{T}_8(^3P_2) | 0 \rangle \right\}.\end{aligned}$$

Phenomenology

- Currently there are no trustable (lattice or experimental) determinations of the P -wave LDMEs $\langle 0 | \mathcal{O}_1(^3P_J) | 0 \rangle$, $\langle 0 | \mathcal{P}_1(^3P_J) | 0 \rangle$ and $\langle 0 | \mathcal{T}_8(^3P_J) | 0 \rangle$
- This is why the impact of the new corrections on the production cross sections has large uncertainties.

Methodology

- To our knowledge, this is the first production calculation where matching coefficients of LDMEs involving chromoelectric fields were *explicitly computed* in the matching between QCD and NRQCD.



Notation

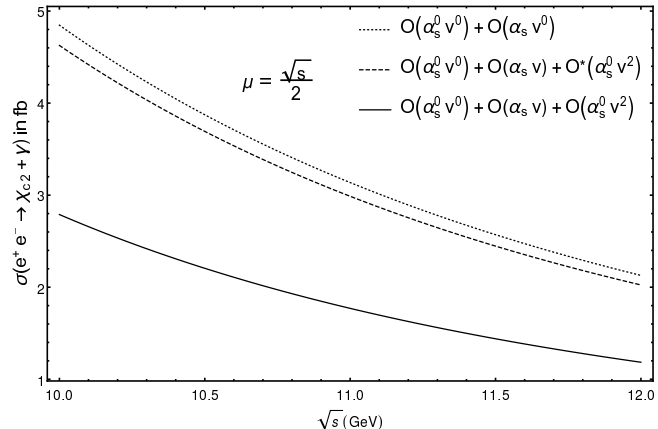
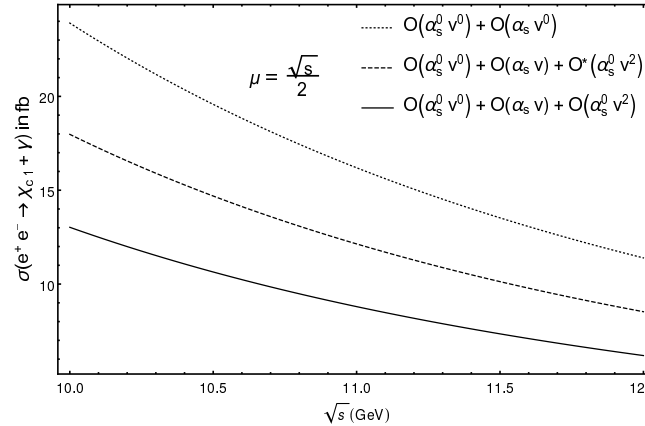
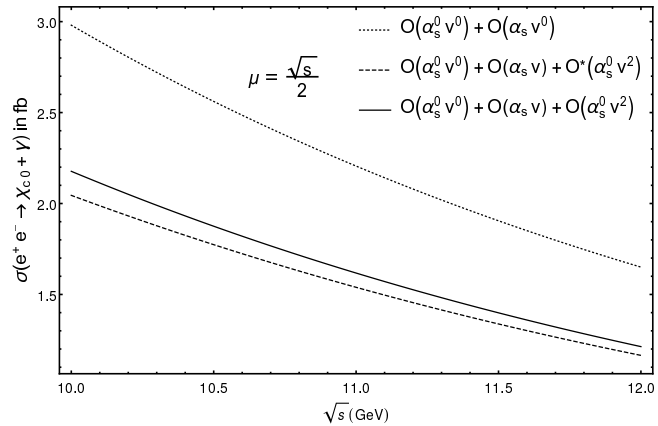
- Explicit values of $C_j^i(r)$ can be found in [Sang & Chen, 2010]
- e_Q is the heavy quark charge
- s is the CM energy
- $r = 4m^2/s$

Matching

- We used factorization at the amplitude level [Braaten & Chen, 1998, Braaten & Lee, 2003] and threshold expansion method [Braaten & Chen, 1996]
- The calculations were carried out both in the CM frame and in the rest frame of the heavy quarkonium (to cross-check our results)

1.1 Numerical results

We fix the matrix elements with the Gremm–Kapustin relation
 → requires binding energy and $\Gamma(\chi_{c0} \rightarrow \gamma\gamma)$



	$\mathcal{O}(\alpha_s^0 v^0)$ and $\mathcal{O}(\alpha_s v^0)$	$\mathcal{O}(\alpha_s^0 v^0)$, $\mathcal{O}(\alpha_s v^0)$ and $\mathcal{O}^*(\alpha_s^0 v^2)$	$\mathcal{O}(\alpha_s^0 v^0)$, $\mathcal{O}(\alpha_s v^0)$ and $\mathcal{O}(\alpha_s^0 v^2)$	$\frac{\sigma_8}{\sigma_1} - 1$
$\sigma(\chi_{c0})$	$(2.49 \pm 0.20 \pm 0.06)$	$(1.72 \pm 0.14 \pm 0.06)$	$(1.82 \pm 0.14 \pm 0.06)$	5.6%
$\sigma(\chi_{c1})$	$(18.8 \pm 1.15 \pm 1.22)$	$(14.1 \pm 0.82 \pm 1.22)$	$(10.2 \pm 1.20 \pm 1.22)$	-27.6%
$\sigma(\chi_{c2})$	$(3.71 \pm 0.19 \pm 1.38)$	$(3.54 \pm 0.17 \pm 1.38)$	$(2.11 \pm 0.39 \pm 1.38)$	-40.4%

for $\sqrt{s} = 10.6$ GeV and $\mu = \sqrt{s}/2$

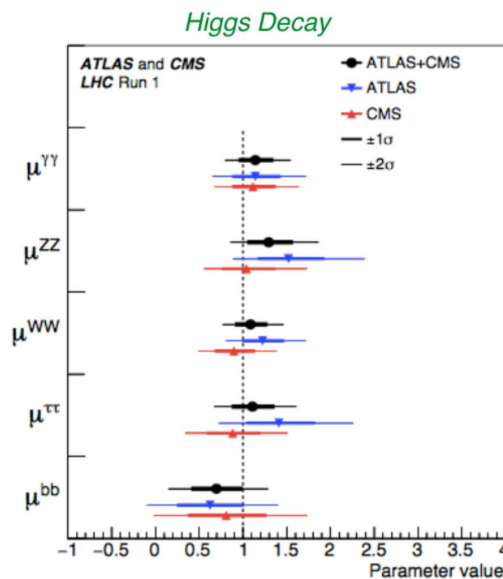
1.2 Quarkonium production in Higgs decay: $H \rightarrow J/\psi + \gamma$

Authors: Nora Brambilla (TUM) Wai Kin Lai (TUM)
Vladyslav Shtabovenko (TUM) Antonio Vairo (TUM)

Report: work in progress

1.2 Motivation

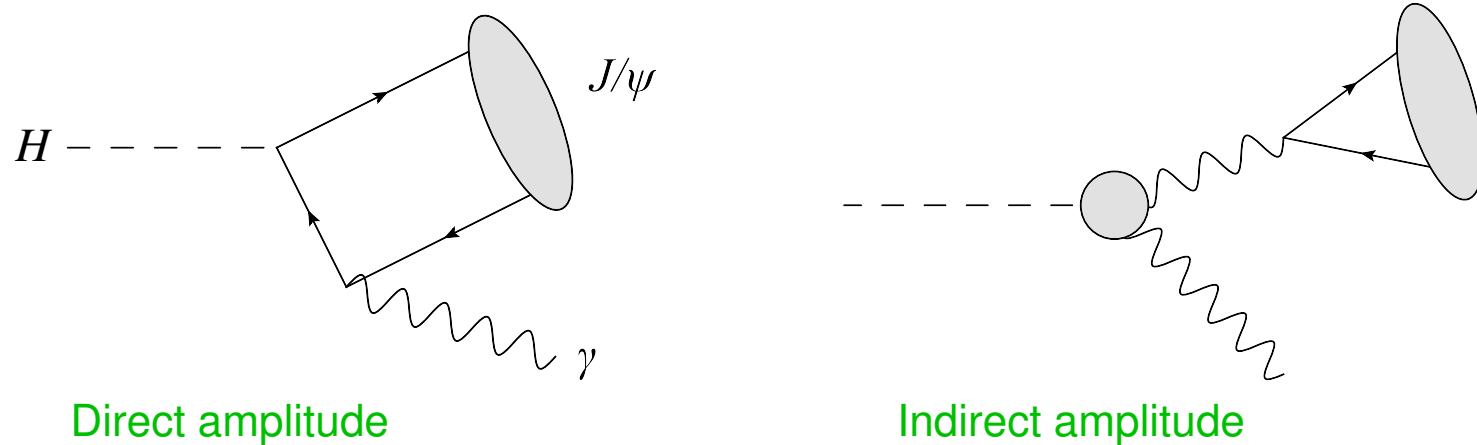
- Measurement of Higgs couplings to other particles eagerly awaited.



$\mu^f = B^f / B_{SM}^f$ measured from LHC Run 1.

- $Hc\bar{c}$ coupling not yet observed.
- $H \rightarrow J/\psi + \gamma$ clean channel to measure $Hc\bar{c}$ coupling.
- Precision calculation of $H \rightarrow J/\psi + \gamma$ decay rate needed.

1.2 Quarkonium production mechanisms in Higgs decay



- Indirect amplitude determined to percent level.
- Direct amplitude has large uncertainties. State of the art: $\mathcal{O}(v^2)$ and $\mathcal{O}(\alpha_s)$. See Bodwin Chung Ee Lee Petriello PR D90 (2014) 113010.
- Aim of this project: $\mathcal{O}(v^4)$ corrections to direct amplitude with light-cone resummation.

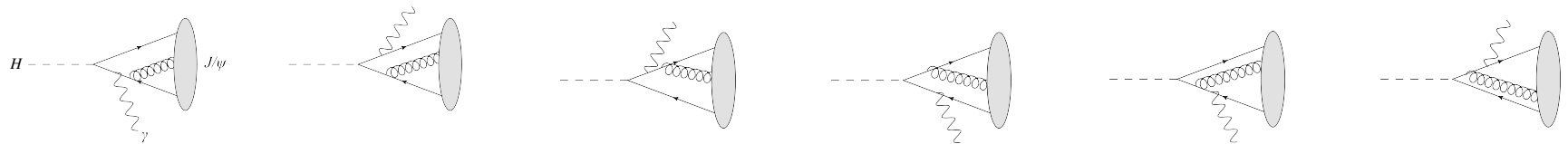
1.2 Light-cone distribution amplitude

Computations may be performed using the light-cone approach ...

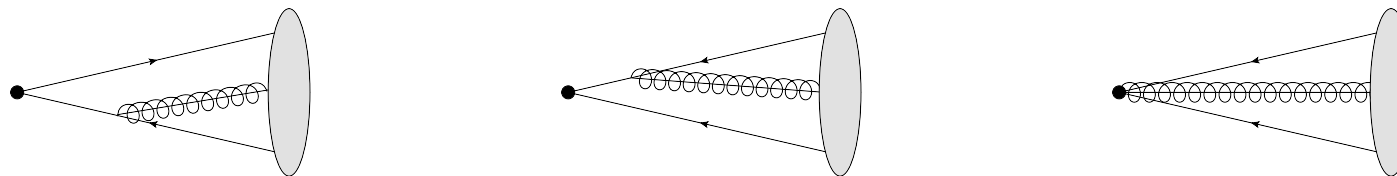
Light-cone distribution amplitude (LCDA) $\phi_V^\perp(x)$:

$$\frac{1}{2} \langle V | \bar{Q}(z)[\gamma^\mu, \gamma^\nu][z, 0]Q(0) | 0 \rangle = f_V (\epsilon_V^{*\mu} p_V^\nu - \epsilon_V^{*\nu} p_V^\mu) \int_0^1 dx e^{ip_V^- zx} \phi_V^\perp(x)$$

- QCD-LCDA factorization for $Q\bar{Q}g$ final state at LO in α_s in the light-cone limit:



Diagrams for the LCDA with $Q\bar{Q}g$ final state:



1.2 Light-cone distribution amplitude

- The amplitude reads

$$i\mathcal{M} = \frac{i}{2} ee_Q \kappa_Q m (\sqrt{2} G_F)^{1/2} f_V \left(-\epsilon_V^* \cdot \epsilon_\gamma^* + \frac{\epsilon_V^* \cdot p_\gamma \epsilon_\gamma^* \cdot p_V}{p_\gamma \cdot p_V} \right) \int_0^1 dx \frac{1}{x(1-x)} \phi_V^\perp(x)$$

- The running of $\phi_V^\perp(x, \mu)$ is governed by the Brodsky–Lepage kernel:

$$\mu^2 \frac{\partial}{\partial \mu^2} \phi_V^\perp(x, \mu) = C_F \frac{\alpha_s(\mu)}{4\pi} \int_0^1 dy V_T(x, y) \phi_V^\perp(y, \mu)$$

that allows to resum $\log^n(m_H/m_Q)$.

1.2 NRQCD matrix elements

... or in NRQCD.

Relevant matrix elements up to $\mathcal{O}(v^4)$ are

LDME (abbrev.)	LDME	relative order
ϕ_0	$\frac{1}{\sqrt{2N_c}} \langle V \psi^\dagger \boldsymbol{\sigma} \cdot \boldsymbol{\epsilon} \chi 0 \rangle$	1
$\langle v^2 \rangle$	$\frac{1}{m_Q^2 \sqrt{2N_c} \phi_0} \langle V \psi^\dagger \boldsymbol{\sigma} \cdot \boldsymbol{\epsilon} (-\frac{i}{2} \overleftrightarrow{D})^2 \chi 0 \rangle$	v^2
$\langle O_2 \rangle$	$\frac{1}{m_Q^2 \sqrt{2N_c} \phi_0} \langle V \psi^\dagger \sigma^i \epsilon^j (-\frac{i}{2})^2 \overleftrightarrow{D}^{(i} \overleftrightarrow{D}^{j)} \chi 0 \rangle$	v^4
$\langle v^4 \rangle$	$\frac{1}{m_Q^4 \sqrt{2N_c} \phi_0} \langle V \psi^\dagger \boldsymbol{\sigma} \cdot \boldsymbol{\epsilon} (-\frac{i}{2} \overleftrightarrow{D})^4 \chi 0 \rangle$	v^4
$\langle O_B \rangle$	$\frac{1}{m_Q^2 \sqrt{2N_c} \phi_0} \langle V \psi^\dagger g \mathbf{B} \cdot \boldsymbol{\epsilon} \chi 0 \rangle$	v^3
$\langle O_{E1} \rangle$	$\frac{1}{m_Q^3 \sqrt{2N_c} \phi_0} \langle V \psi^\dagger (\boldsymbol{\sigma} \times (g \mathbf{E} \times \overleftrightarrow{D})) \cdot \boldsymbol{\epsilon} 0 \rangle$	v^3
$\langle O_{E2} \rangle$	$\frac{1}{m_Q^3 \sqrt{2N_c} \phi_0} \langle V \psi^\dagger \boldsymbol{\sigma} \cdot \boldsymbol{\epsilon} (\overleftrightarrow{D} \cdot g \mathbf{E} - g \mathbf{E} \cdot \overleftrightarrow{D}) \chi 0 \rangle$	v^3
$\langle O_{E3} \rangle$	$\frac{1}{m_Q^3 \sqrt{N_c} \phi_0} \langle V \psi^\dagger (\boldsymbol{\sigma} \cdot g \mathbf{E}) \boldsymbol{\epsilon} \cdot \overleftrightarrow{D} \chi 0 \rangle$	v^3

that match the corresponding LCDA (ϕ_0 is the quarkonium wave-function at the origin):

$$f_V = \frac{\sqrt{N_c m_V}}{m_Q} \phi_0 \left(1 - \frac{5}{6} \langle v^2 \rangle + \frac{19}{24} \langle v^4 \rangle \right)$$

$$f_V \int_0^1 dx (2x-1)^2 \phi_V^\perp(x) = -\frac{1}{2} \langle v^2 \rangle + \frac{3}{10} \langle O_2 \rangle - \langle O_B \rangle + \frac{3}{5} \langle O_{E1} \rangle + \frac{13}{40} \langle O_{E2} \rangle - \frac{9}{20} \langle O_{E3} \rangle$$

$$f_V \int_0^1 dx (2x-1)^4 \phi_V^\perp(x) = \frac{43}{120} \langle v^4 \rangle$$

2. Quarkonium-Quarkonium Interaction

2. Atom-Atom and Quarkonium-Quarkonium Interaction

Authors: Nora Brambilla (TUM) Vladyslav Shtabovenko (TUM)
Jaume Tarrús Castellà (TUM) Antonio Vairo (TUM)

Report: TUM-EFT 58/14

Journal: Phys. Rev. D95 (2017) no.11, 116004

Authors: Nora Brambilla (TUM) Gastão Krein (U. São Paolo)
Jaume Tarrús Castellà (TUM) Antonio Vairo (TUM)

Report: TUM-EFT 70/15

Journal: Phys. Rev. D93 (2016) no.5, 054002

2.1 Van der Waals interaction in QED

Atom-atom interactions are characterized by several energy scales ($m = \text{mass of } e^-$): $a_0 \sim 1/(m\alpha)$ (Bohr radius), $E \sim m\alpha^2$ (atomic binding energy), R (atom-atom distance), $W, T \sim Q$ (potential, kinetic energy between atoms).

We have studied the atom-atom van der Waals interactions in the

- short-range regime $1/E \gg R \gg a_0$, also known as the London limit

$$W_{\text{Lon}} \sim 1/R^6$$

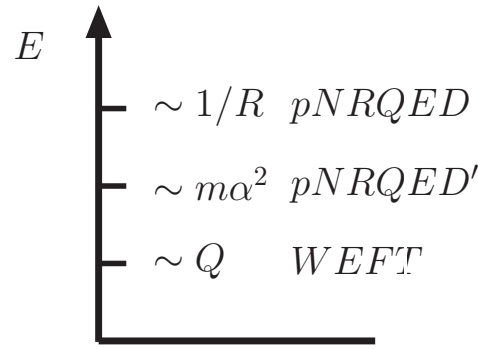
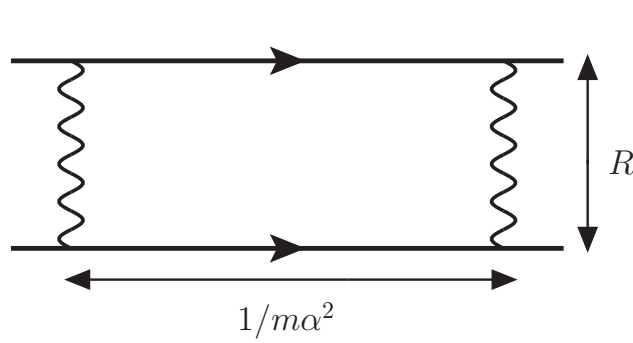
- long-range regime $R \gg 1/E \gg a_0$, also known as the Casimir–Polder limit

$$W_{\text{CP}} \sim 1/R^7$$

- intermediate regime $R \sim 1/E \gg a_0$.

using an EFT framework that allows to explicitly construct a van der Waals EFT (WEFT).

2.1 Short-range van der Waals static potential



Defining $\Delta E_{nm} = E_n - E_m$ and x, μ the electron orbital radius and magnetic moment

$$p_E(n, m) = \frac{e^2}{3} \langle n | \mathbf{x} | m \rangle \cdot \langle m | \mathbf{x} | n \rangle$$

which is related to the static electric polarizability ($\alpha_n = \sum' m p_E(n, m) / (2\pi\Delta E_{nm})$), the LO van der Waals potential (London limit) reads

$$W^{\text{LO}} = W_{\text{Lon}} = \frac{3}{8\pi^2 R^6} \sum'_{m_1, m_2} \frac{p_E(n_1, m_1) p_E(n_2, m_2)}{\Delta E_{n_1 m_1} + \Delta E_{n_2 m_2}}$$

2.1 Short-range van der Waals static potential: higher orders

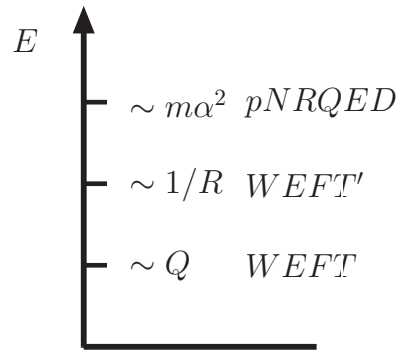
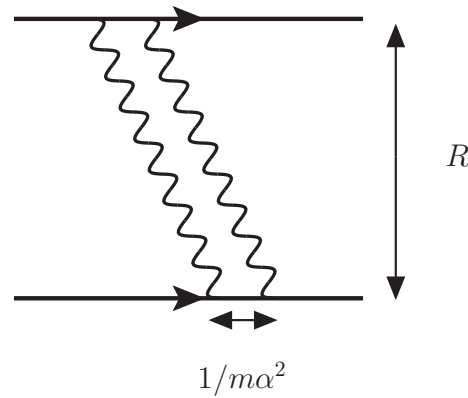
Higher-order corrections to the potential are (counting $1/R \sim m\alpha^{3/2}$ for convenience):

$$\begin{aligned}
 W^{\text{LO} \times \sqrt{\alpha}} &= \frac{\alpha}{m^2} \left[\frac{2\pi}{3} \delta^{(3)}(\mathbf{R}) \langle n_1 | \boldsymbol{\mu} | n_1 \rangle \cdot \langle n_2 | \boldsymbol{\mu} | n_2 \rangle + \frac{3}{4R^3} \hat{\mathbf{R}} \cdot \langle n_1 | \boldsymbol{\mu} | n_1 \rangle \hat{\mathbf{R}} \cdot \langle n_2 | \boldsymbol{\mu} | n_2 \rangle \right] \\
 W^{\text{NLO}} &= -\frac{1}{8\pi^2 R^4} \sum'_{m_1, m_2} p_E(n_1, m_1) p_E(n_2, m_2) \frac{\Delta E_{n_1 m_1} \Delta E_{n_2 m_2}}{\Delta E_{n_1 m_1} + \Delta E_{n_2 m_2}} \\
 W^{\text{NLO} \times \sqrt{\alpha}} &= -\frac{7\alpha^2}{6\pi m^2 R^3} + \dots
 \end{aligned}$$

Terms in $W^{\text{NLO} \times \sqrt{\alpha}}$ carry divergences. After $\overline{\text{MS}}$ subtraction the residual scale dependence cancels against the one in the contact 4-fermion terms of NRQED:

$$W^{\text{NLO} \times \sqrt{\alpha}} \Big|_{\log \nu} = \frac{8\alpha^2}{3m^2} \log \nu - \frac{14\alpha^2}{3m^2} \log \nu + \frac{2\alpha^2}{m^2} \log \nu = 0$$

2.1 Long-range van der Waals static potential



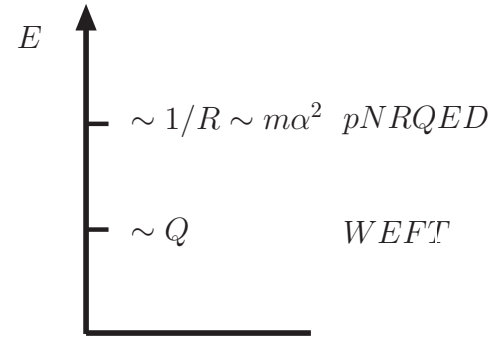
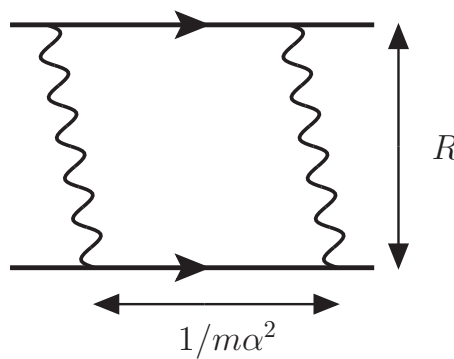
The first non-contact term appears at N^3LO (counting $1/R \sim m\alpha^{5/2}$ for convenience):

$$W^{N^3LO} = W_{CP} = -\frac{23}{4\pi R^7} \alpha_{n_1} \alpha_{n_2} + \dots$$

which corresponds to the [van der Waals potential in the Casimir–Polder limit](#).

Divergences affect single contact terms and the 1-loop diagram leading to the Casimir–Polder potential; all these divergences cancel with each others as in the short-distance case.

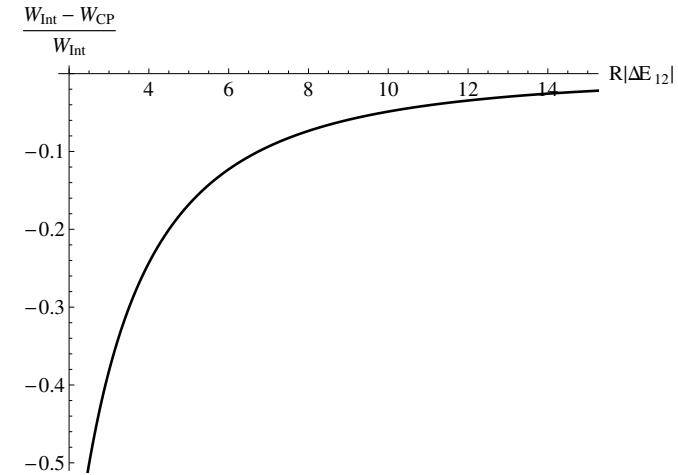
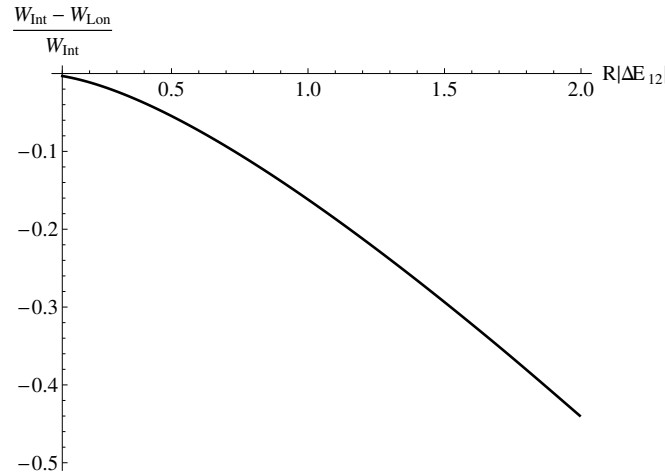
2.1 Intermediate-range van der Waals static potential



The first non-contact term appears at NLO and admits a dispersive representation:

$$\begin{aligned}
 W^{\text{NLO}} = W_{\text{Int}} &= \frac{1}{2\pi^2 R} \lim_{\eta \rightarrow 0} \int_0^\infty d\mu e^{-\mu R} \mu \text{Im} [\widetilde{W}(\eta - i\mu)] \\
 \text{Im} [\widetilde{W}(\eta - i\mu)] &= - \sum'_{m_1, m_2} \frac{p_E(n_1, m_1) p_E(n_2, m_2)}{16\pi} \left\{ 4\Delta E_{n_1 m_1} \Delta E_{n_2 m_2} \right. \\
 &\quad + \frac{\mu^4 + 4\mu^2 \Delta E_{n_1 m_1}^2 + 8\Delta E_{n_1 m_1}^4}{\mu (\Delta E_{n_1 m_1}^2 - \Delta E_{n_2 m_2}^2)} \Delta E_{n_2 m_2} \arccot \left(\frac{2|\Delta E_{n_1 m_1}|}{\mu} \right) \\
 &\quad \left. - \frac{\mu^4 + 4\mu^2 \Delta E_{n_2 m_2}^2 + 8\Delta E_{n_2 m_2}^4}{\mu (\Delta E_{n_1 m_1}^2 - \Delta E_{n_2 m_2}^2)} \Delta E_{n_1 m_1} \arccot \left(\frac{2|\Delta E_{n_2 m_2}|}{\mu} \right) \right\}
 \end{aligned}$$

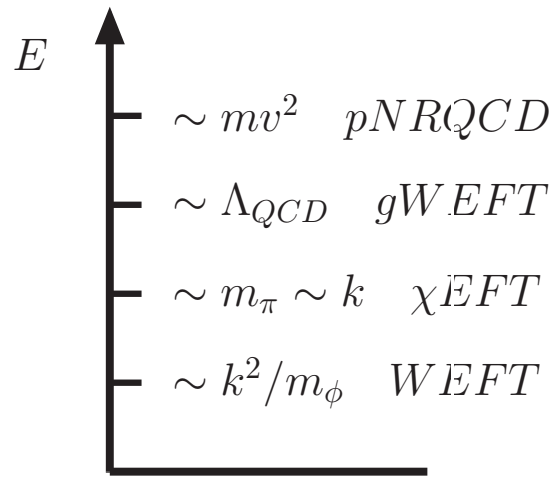
2.1 Intermediate-range van der Waals static potential



Relative difference between the intermediate-range van der Waals potential with the London potential and the Casimir–Polder potential for both atoms in the ground state.

The London potential and the Casimir–Polder potential are a good approximation in the short and long distances respectively. Due to a conspiracy of numerical factors and cancellations, the convergence towards the London potential is somewhat faster than the one towards the Casimir–Polder potential.

2.2 Quarkonium-quarkonium van der Waals static potential

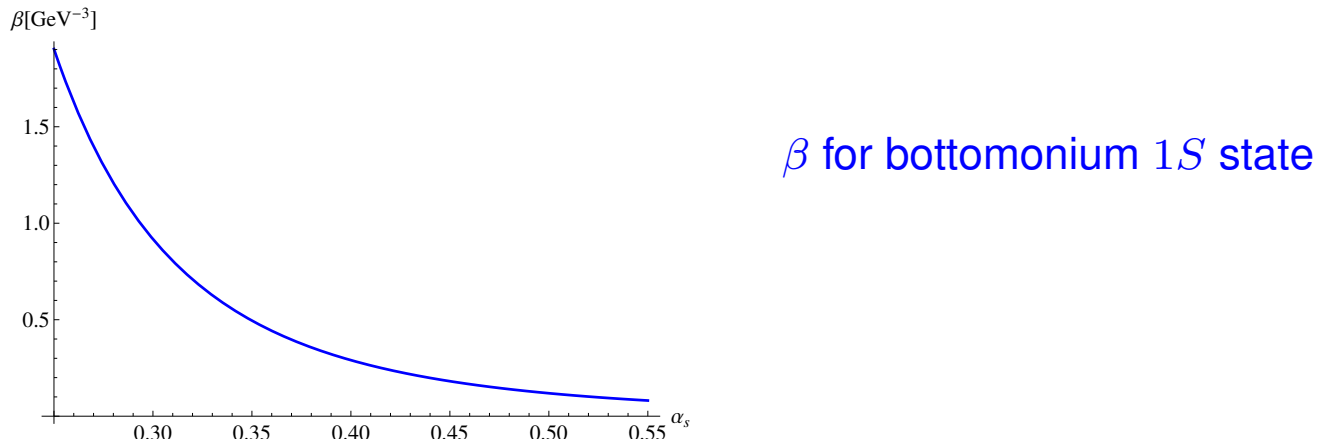


The hierarchy of scales and the sequence of EFTs is similar to the QED case.

In the long-range the interaction is non-perturbative and governed by a **polarizability coupling β** and the **two-pion production** by the polarizability operator.

2.2 Polarizability and two-pion production

- For the quarkonium ground state the **polarizability coupling** may be computed in PT:



- In the low-energy limit the **two-pion production** by the polarizability operator is determined up to a constant from **chiral algebra** and the **QCD anomaly in the trace of the energy-momentum tensor**:

$$g^2 \langle \pi^+(p_1) \pi^-(p_2) | \mathbf{E}_a^2 | 0 \rangle = \frac{8\pi^2}{b} (\kappa_1 p_1^0 p_2^0 - \kappa_2 p_1^i p_2^i + 3m_\pi^2)$$

where $\kappa_1 = 2 - 9\kappa/2$, $\kappa_2 = 2 + 3\kappa/2$, b is the first coefficient of the beta function, and $\kappa = 0.186 \pm 0.003 \pm 0.006$ from BES coll. PR D62 (2000) 032002.

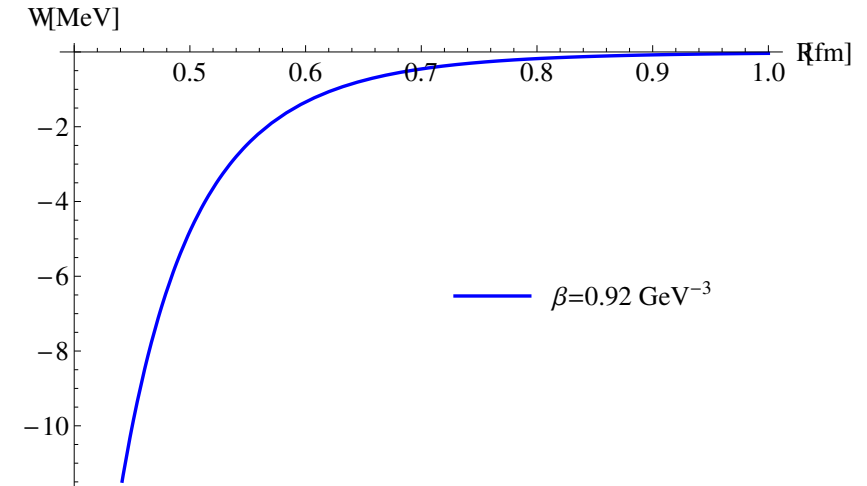
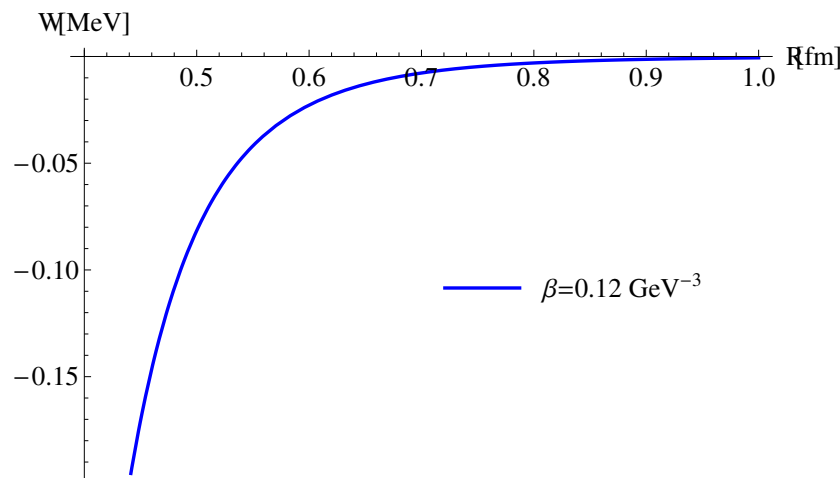
2.2 Quarkonium-quarkonium van der Waals static potential

$$\begin{aligned}
 W &= -\frac{3\pi\beta^2 m_\pi^2}{8b^2 R^5} \left[\left(4(\kappa_2 + 3)^2 (m_\pi R)^3 + (3\kappa_1^2 + 43\kappa_2^2 + 14\kappa_1\kappa_2) m_\pi R \right) K_1(2m_\pi R) \right. \\
 &\quad \left. + 2(2(\kappa_2 + 3)(\kappa_1 + 5\kappa_2)(m_\pi R)^2 + (3\kappa_1^2 + 43\kappa_2^2 + 14\kappa_1\kappa_2)) K_2(2m_\pi R) \right] \\
 &\underset{Rm_\pi \gg 1}{\approx} -\frac{3(3 + \kappa_2)^2 \pi^{3/2} \beta^2}{4b^2} \frac{m_\pi^{9/2}}{R^{5/2}} e^{-2m_\pi R}
 \end{aligned}$$

where K_n are modified Bessel functions of the second kind.

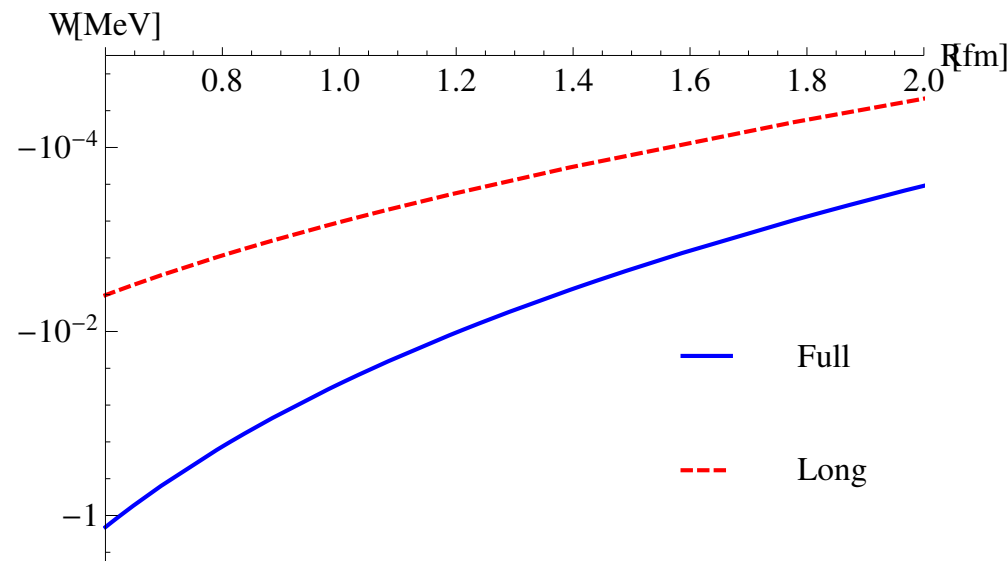
The result completes previous findings by Fujii Kharzeev PR D60 (1999) 114039.

For the 1S-1S bottomonium van der Waals static potential we obtain:



2.2 Full vs long-range potential

For the **1S-1S bottomonium van der Waals static potential** the impact of chiral corrections to the long-range limit is sizeable and attractive.



2.3 Chiral corrections to the quarkonium mass

As a side-product of having established the leading pion- $1S$ -quarkonium coupling one can determine the **leading chiral logarithm of the $1S$ quarkonium mass**, which reads

$$\delta m_{\text{quarkonium}}|_{\text{chiral log}} = -\frac{3}{8} \frac{\beta}{b} m_\pi^4 \log \frac{m_\pi^2}{\nu^2}$$

This result corrects Grinstein Rothstein PL B385 (1996) 265.

3. Quarkonium interaction with light d.o.f.

3. Quarkonium interaction with light degrees of freedom

Authors: Nora Brambilla (TUM) Gastão Krein (U. São Paolo)
Jaume Tarrús Castellà (TUM) Antonio Vairo (TUM)

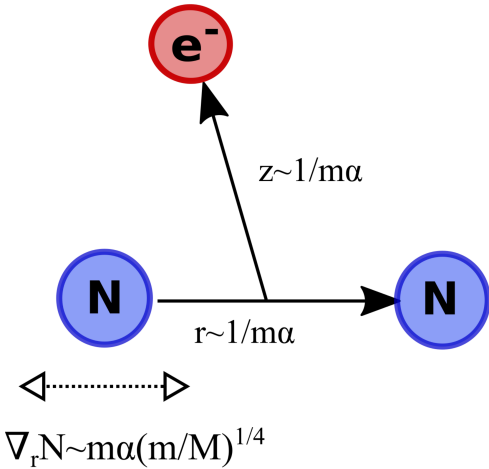
Report: TUM-EFT 69/15

Journal: submitted to Phys. Rev. D

→ see the project A3 report of Wai Kin Lai for the QCD applications.

3.1 Energy scales in a H_2^+ -like molecule

$$E_{\text{heavy}} \sim m\alpha^2(m/M)^{1/2} \quad E_{\text{light}} \sim m\alpha^2$$



The typical energy scales in a H_2^+ -like molecule are:

$r \sim z \sim 1/(m\alpha)$ (size of the atom and molecule), $E \sim m\alpha^2$ (atomic binding energy), E_{heavy} (energy of the molecular vibrational modes)

These scales are hierarchically ordered (m is the electron mass $\ll M$ the nuclei mass).

From the virial theorem applied to the vibrational modes it follows: $E_{\text{heavy}} \sim m\alpha^2 \sqrt{\frac{m}{M}}$.

The Born–Oppenheimer EFT (BOEFT) is the EFT that describes these modes, Ψ_κ .

3.1 Born–Oppenheimer EFT in QED

$$\begin{aligned} L_{\text{BOEFT}} = & -\frac{1}{4} \int d^3x F_{\mu\nu}(x) F^{\mu\nu}(x) \\ & + \int d^3r \sum_{\kappa} \Psi_{\kappa}^{\dagger}(t, \mathbf{r}) \{ [i\partial_t + e_{\text{tot}} A_0(t, \mathbf{0}) - H_{\kappa}^{(0)}(\mathbf{r}) - \delta E_{\kappa}(\mathbf{r})] \Psi_{\kappa}(t, \mathbf{r}) \\ & - \int d^3r \sum_{\kappa\kappa'} \Psi_{\kappa}^{\dagger}(t, \mathbf{r}) C_{\kappa\kappa'}^{\text{nad}}(\mathbf{r}) \Psi_{\kappa'}(t, \mathbf{r}) \end{aligned}$$

The operator $H_{\kappa}^{(0)}$ is the LO nuclei-nuclei Hamiltonian:

$$H_{\kappa}^{(0)}(\mathbf{r}) = -\frac{\nabla_r^2}{M} + V_{ZZ}^{\text{LO}}(\mathbf{r}) + V_{\kappa}^{\text{light}}(\mathbf{r})$$

V_{ZZ}^{LO} is the LO nuclei-nuclei electromagnetic potential,

$V_{\kappa}^{\text{light}}$ is the Born–Oppenheimer potential.

3.1 Born–Oppenheimer potentials

The Born–Oppenheimer potentials are solutions of the Schrödinger equation

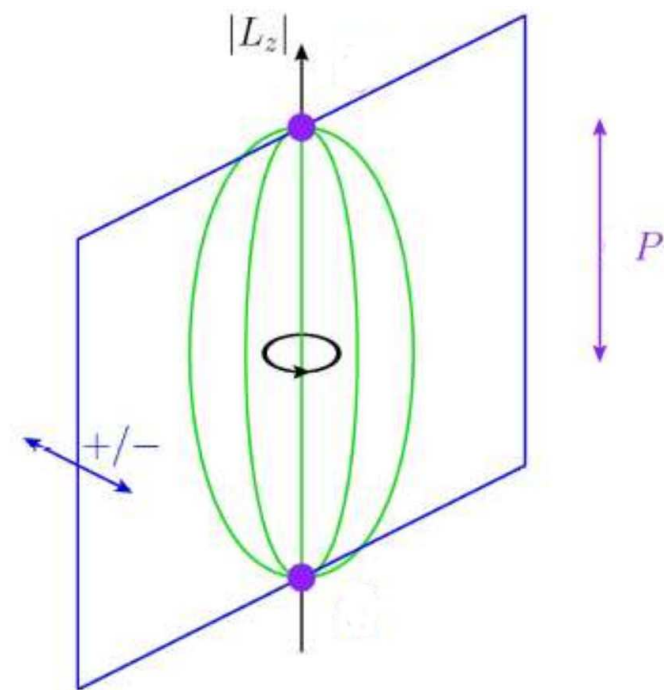
$$\left[-\frac{\nabla_z^2}{2m} + V_{Ze}^{\text{LO}}(z + r/2) + V_{Ze}^{\text{LO}}(z - r/2) \right] \phi_\kappa(\mathbf{r}; z) = V_\kappa^{\text{light}}(\mathbf{r}) \phi_\kappa(\mathbf{r}; z).$$

where V_{Ze}^{LO} is the LO nuclei-electron electromagnetic potential.

The label κ reflects the cylindrical symmetry of the system.

Representations labeled Λ_η^σ

- ▶ Λ rotational quantum number
 $|\hat{\mathbf{n}} \cdot \mathbf{K}| = 0, 1, 2 \dots$ corresponds to
 $\Lambda = \Sigma, \Pi, \Delta \dots$
- ▶ η eigenvalue of \hat{P} :
 $g \hat{=} +1$ (gerade), $u \hat{=} -1$ (ungerade)
- ▶ σ eigenvalue of reflections
- ▶ σ label only displayed on Σ states
(others are degenerate)



3.1 Higher-order Born–Oppenheimer potentials

$$\delta E_\kappa(\mathbf{r}) = \delta^{\text{rec}} E_\kappa(\mathbf{r}) + \delta^{\text{rec}, 2} E_\kappa(\mathbf{r}) + \delta^{\text{NLO}} E_\kappa(\mathbf{r}) + \delta^{\text{US}} E_\kappa(\mathbf{r}) + \dots$$

contains higher-order contributions to the Born–Oppenheimer potential,
e.g., the nucleus recoil correction

$$\delta^{\text{rec}} E_\kappa(\mathbf{r}) = \int d^3z \phi_\kappa^*(\mathbf{r}; \mathbf{z}) \left(-\frac{\nabla_z^2}{4M} \right) \phi_\kappa(\mathbf{r}; \mathbf{z})$$

or iteration of it, $\delta^{\text{rec}, 2} E_\kappa$, or NLO electromagnetic corrections to the potential, $\delta^{\text{NLO}} E_\kappa$,
or Lamb-shift-like corrections

$$\begin{aligned} \delta^{\text{US}} E_\kappa(\mathbf{r}) &= -\frac{e^2}{6\pi^2} \left\{ -\frac{Ze^2}{2m^2} \left[\log\left(\frac{\mu}{m}\right) + \frac{5}{6} - \log(2) \right] \rho_\kappa(\mathbf{r}) \right. \\ &\quad + \sum_{\bar{\kappa} \neq \kappa} \left| \int d^3z \phi_\kappa^*(\mathbf{r}; \mathbf{z}) \left(-i \frac{\nabla_z}{m} \right) \phi_{\bar{\kappa}}(\mathbf{r}; \mathbf{z}) \right|^2 (V_\kappa^{\text{light}}(\mathbf{r}) - V_{\bar{\kappa}}^{\text{light}}(\mathbf{r})) \right. \\ &\quad \times \left. \log\left(\frac{m}{|V_\kappa^{\text{light}}(\mathbf{r}) - V_{\bar{\kappa}}^{\text{light}}(\mathbf{r})|}\right) \right\} \end{aligned}$$

where $\rho_\kappa(\mathbf{r})$ is the electron density at the positions of the nuclei.

3.1 Non-adiabatic couplings

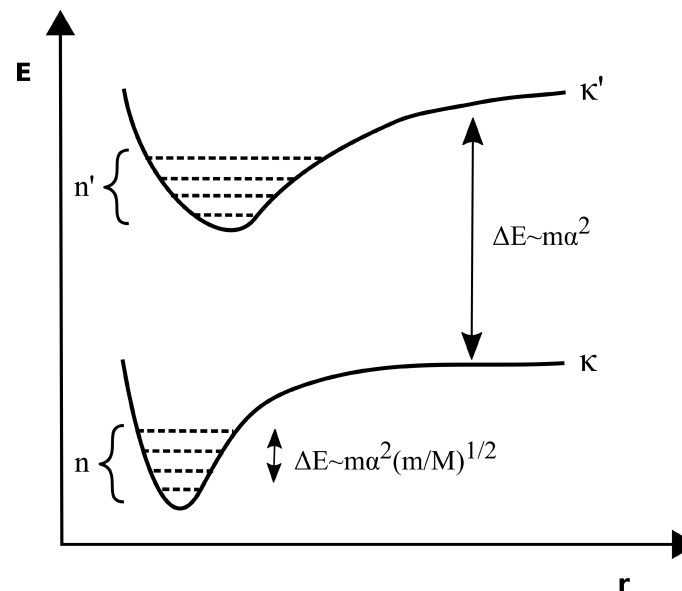
$C_{\kappa\kappa'}^{\text{nad}}(\mathbf{r})$ is the nonadiabatic coupling:

$$C_{\kappa\kappa'}^{\text{nad}}(\mathbf{r}) = \int d^3z \phi_\kappa^*(\mathbf{r}; \mathbf{z}) [-\nabla_r^2/M, \phi_{\kappa'}(\mathbf{r}; \mathbf{z})]$$

It is responsible for the mixing between Born–Oppenheimer levels.

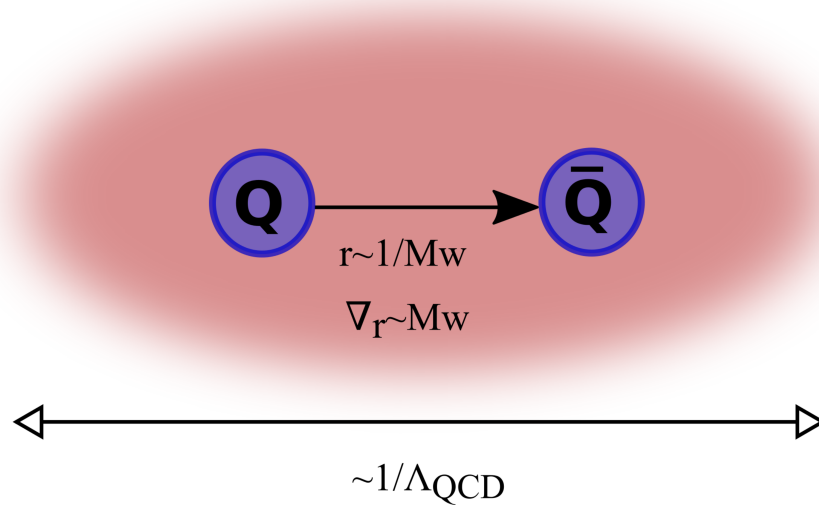
In the molecular case, this mixing is suppressed → suppression of the Λ doubling.

Molecular energy levels:



3.2 Born–Oppenheimer EFT in QCD

$$E_{\text{heavy}} \sim M_w^2 \quad E_{\text{light}} \sim \Lambda_{\text{QCD}}$$



Adjoint quarkonium bound with gluons (**hybrids**) or with light quarks (**tetraquarks**) is a system very similar to the H_2^+ molecule, but with some noteworthy differences:

- The size of the hadron is $1/\Lambda_{\text{QCD}}$, but the $Q\bar{Q}$ distance, $1/(Mw)$, is smaller.
- In the short distance the cylindrical symmetry becomes a much stronger spherical symmetry, with a specific pattern of degeneracies.
- The nonadiabatic coupling may count for nearly degenerate states as the LO Born–Oppenheimer potential \rightarrow strong Λ doubling.

→ see [project A3](#).

Outlook

Consistently with the two years funding we plan to complete the following items.

- Full $\mathcal{O}(\alpha_s v^2)$ phenomenological analysis of $H \rightarrow J/\psi + \gamma$ with complete error budget. In particular, we will carefully size the effect of the octet matrix elements (of similar nature to those appearing in $e^+e^- \rightarrow \chi_{cJ} + \gamma$).
- The polarizability coupling and operator entering quarkonium-quarkonium van der Waals interactions are also crucial ingredients in quarkonium hadronic transitions and in particular in dipion transitions. We will study in a suitable EFT framework these observables.